Excited-State Behavior of *N*-Phenyl-Substituted *trans*-3-Aminostilbenes: Where the "*m*-Amino Effect" Meets the "Amino-Conjugation Effect"

Jye-Shane Yang,* Kang-Ling Liau, Chi-Wei Tu, and Chung-Yu Hwang

Department of Chemistry, National Central University, Chung-Li 32054, Taiwan

Received: April 6, 2005; In Final Form: June 5, 2005

The electronic spectroscopy and photochemistry of the trans isomers of 3-(*N*-phenylamino)stilbene (**m1c**), 3-(*N*-methyl-*N*-phenylamino)stilbene (**m1d**), 3-(*N*,*N*-diphenylamino)stilbene (**m1e**), and 3-(*N*-(2,6-dimethylphenyl)amino)stilbene (**m1f**) and their double-bond constrained analogues **m2a**−**m2c** and **m2e** are reported. When compared with *trans*-3-aminostilbene (**m1a**), **m1c**−**m1e** display a red shift of the $S_0 \rightarrow S_1$ absorption and fluorescence spectra, lower oscillator strength and fluorescence rate constants, and more efficient $S_1 \rightarrow T_1$ intersystem crossing. Consequently, the *N*-phenyl derivatives **m1c**−**m1e** have lower fluorescence quantum yields and higher photoisomerization quantum yields. The corresponding *N*-phenyl substituent effect in **m2a**−**m2e** is similar in cyclohexane but smaller in acetonitrile. This is attributed to the weaker intramolecular charge transfer character for the S_1 state of **m2** so that the rates for intersystem crossing are less sensitive to solvent polarity. It is also concluded that *N*-phenyl substitutions do not change the triplet mechanism of photoisomerization for **m1** in both nonpolar and polar solvents. Therefore, the "*m*-amino conjugation effect" reinforces the "*m*-amino effect" on fluorescence by further reducing its rate constants and highlights the *N*-phenyl-enhanced intersystem crossing from the "amino-conjugation effect" by making $S_1 \rightarrow T_1$ the predominant nonradiative decay pathway.

Introduction

Stilbene and its derivatives play a crucial role in the current understanding and application of photoinduced trans−cis isomerization of alkenes, one of the most thoroughly investigated reactions in molecular photochemistry.[1,2] The trans → cis double-bond torsion in the lowest singlet excited state (S_1) encounters an energy barrier (E_a) before it reaches a surface minimum at the perpendicular geometry (^{1}p*) (Figure 1).[3,4] The ^{1}p* state then undergoes an efficient surface jump $S_1 \rightarrow S_0$ due to the conical intersection, which accounts for a fraction of ~0.5 for the decay of ^{1}p* to the trans (β) and cis (1-β) isomer (e.g., $\beta = 0.46$ for *trans*-stilbene). Although the corresponding potential-energy surface in the triplet state (T_1) is barrierless, photoisomerization via the triplet state is limited by the inefficient $S_1 \rightarrow T_1$ intersystem crossing, except for some halogen-, nitro-, and carbonyl-substituted derivatives.[1] With disregard for the mechanism, photoisomerization often dominates fluorescence in accounting for the excited decay of *trans*-stilbenes.

The "*m*-amino effect"[5−8] and the "amino-conjugation effect"[9−11] are two of the few substituent effects that could substantially suppress the photoisomerization quantum yield (Φ_{ts}) and thus increase the fluorescence quantum yield (Φ_f) for unconstrained *trans*-stilbenes. The former effect is illustrated by the more than 1 order of magnitude larger Φ_f for *trans*-3-aminostilbene (**m1a**) than for *trans*-4-aminostilbene (**p1a**), which is also an intriguing example of a position-dependent substituent effect in molecular photochemistry.[4,12] The latter effect reflects elongated conjugation for **p1a** by *N*-phenyl substitutions, as exemplified by aminostilbenes **p1c**, **p1d**, and **p1e**. A common feature for these two amino substituent effects

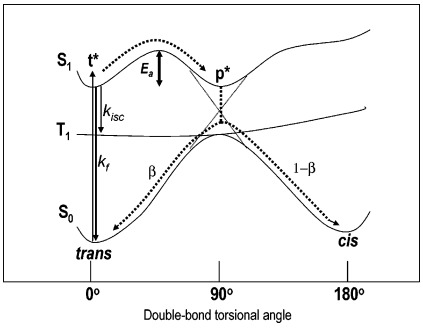

Figure 1. Simplified potential-energy diagram for the lowest electronic states of stilbenes. The dash arrows show the trans → cis photoisomerization pathway along the S_1 state.

is the larger stabilization of the S_1 state vs the ^{1}p* state so that the barrier for the singlet-state torsion is increased and the rate for photoisomerization is reduced. When the torsional barrier is too high to be overcome, photoisomerization occurs only via the triplet state (e.g., **m1a** and **ple**). Therefore, the efficiency of intersystem crossing relative to that of fluorescence becomes crucial in determining the values of Φ_{tc} and Φ_f for these "high-torsion-barrier" *trans*-stilbenes. As compared with the dynamics of **p1a** ($k_f \approx 6 \times 10^8$ s^{-1} and $k_{isc} \approx 4 \times 10^7$ s^{-1}),[6] the $S_1 \rightarrow T_1$ intersystem crossing is more important for **m1a** because the fluorescence rate constant decreases more than the intersystem-crossing rate constant ($k_f \approx 1 \times 10^8$ s^{-1} and $k_{isc} \approx 2.4 \times 10^7$ s^{-1}), but for **p1e** it is mainly due to the lager rate constant for intersystem crossing ($k_f \approx 4 \times 10^8$ s^{-1} and $k_{isc} \approx 3 \times 10^8$ s^{-1}). Apparently, the inherent nature of these two amino substituent effects is different.

In view of the pronounced "*m*-amino effect" and "amino-conjugation effect", it is desired to investigate the corresponding effect of their combinations, namely, the "*m*-amino conjugation

* To whom correspondence may be addressed. E-mail: jsyang@cc.ncu.edu.tw.

10.1021/jp0517807 CCC: $30.25
Published on Web 07/01/2005

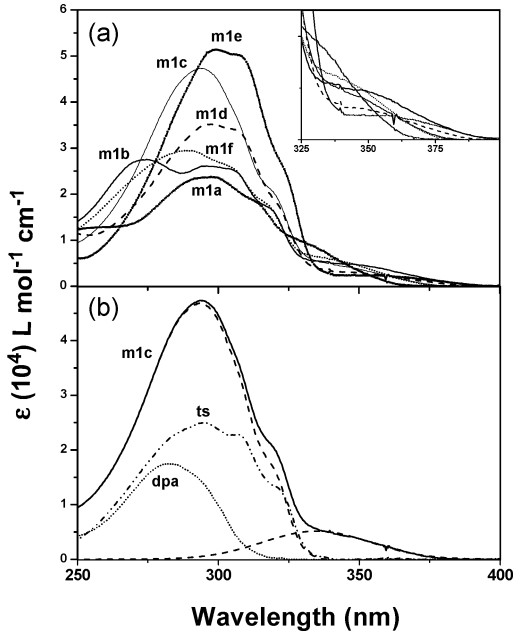

Figure 2. UV−vis absorption spectra of (a) **m1a**−**m1f** with the long-wavelength absorption band amplified (inset) and (b) *trans*-stilbene (ts) and diphenylamine (dpa) in cyclohexane along with Gaussian deconvolutions of the longest wavelength transition in the spectra of **m1c**.

effect", on the photochemistry of *trans*-stilbene. Moreover, the difference in electronic properties between meta- and para-conjugated systems has been a subject of current interest,[13−18] particularly in accounting for their different performance as nonlinear optical,[13] light-harvesting,[14−16] and light-emitting[17,18] materials. In this context, we have investigated the excited-state behavior of *N*-phenyl-substituted *trans*-3-aminostilbenes **mlc**−**m1f** and their double-bond constrained derivatives **m2a**−**m2c** and **m2e**. We report herein that *N*-phenyl substitutions in **m1a** result in smaller fluorescence quantum yields and larger trans → cis photoisomerization quantum yields. The origin of such a *m*-amino conjugation effect will be elucidated and compared with the amino conjugation effect on the para isomers **p1a**−**p1f** and **p2a**−**p2e**.[9,11]

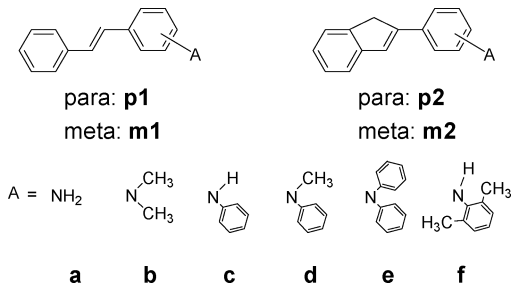

Results

Absorption Spectra. The absorption spectra of **m1c**−**m1f** in cyclohexane are shown in Figure 2a. For comparison, the spectra of **m1a**[6] and **m1b**[7] in cyclohexane are included. As in the cases of **m1a** and **m1b**, **m1c**−**m1f** display multiple absorption bands, with the most intense bands near 300 nm and shoulders of low intensity near 340 nm. The introduction of *N*-substituents in **m1a** results in a hyperchromic shift of the 300-nm bands and a hypochromic shift of the 340-nm bands. The latter is also accompanied with a red shift, whereas there is no specific shift for the former bands. By assumption that the long wavelength 340-nm bands correspond to the $S_0 \rightarrow S_1$ transition, the oscillator strengths (f) were estimated by integrating the deconvoluted Gaussian bands (e.g., **m1c** in Figure 2b). These data along with the absorption maxima for **m1a**−**m1f** in cyclohexane and acetonitrile are reported in Table 1. The oscillator strengths decrease in the order **m1a** > **m1f** > **m1c** ≈ **m1b** > **m1d** > **m1e**, and the wavelength of the lowest energy absorption maxima (λ_{abs}) increases in the order **m1a** < **m1f** ≈ **m1c** < **m1d** < **m1b** < **m1e**. The similarity in both parameters for **m1a** and **m1f** suggests that the differences in f and λ_{abs} among **m1a**−**m1f** are associated with the π-conjugation interactions, since the bulky *N*-aryl group in **m1f** is expected to have the least degree of conjugation with the aminostilbene moiety. Figure 2b also shows the absorption spectra of *trans*-stilbene and diphenylamine in cyclohexane, which are located within the envelope of the 300-nm bands for **m1c**. This appears to indicate that the more allowed upper excited states are of more localized transitions. The small change in absorption maxima for **m1a**−**m1f** on going from cyclohexane to actonitrile also indicates a small difference between the dipole moments of the ground and Franck−Condon excited state.

TABLE 1: Maxima of UV Absorption (λ_{Abs}) and Fluorescence (λ_f), Fluorescence-Band Half-Width ($\Delta\nu_{1/2}$), 0,0 Transition ($\lambda_{0,0}$), Stokes Shifts ($\Delta\nu_{st}$), and Oscillator Strength (f) for the $S_0 \rightarrow S_1$ Band of m1 and m2 in Cyclohexane (c-Hex) and Acetonitrile (MeCN)[a]

compd	solvent	λ_{abs} (nm)[b]	λ_f (nm)[c]	$\Delta\nu_{1/2}$ (cm^{-1})	$\lambda_{0,0}$ (nm)[d]	$\Delta\nu_{st}$ (cm^{-1})[e]	f[f]
m1a	c-Hex	297 (328)	(378) 394	4114	359 (354)	5107	0.14
	MeCN	298 (330)	456	4266	384	8373	0.15
m1b	c-Hex	296 (344)	(400) 416	3665	382 (370)	5031	0.09
	MeCN	297 (344)	490	4029	410	8662	0.09
m1c	c-Hex	294 (335)	(388) 403	3716	371 (369)	5037	0.10
	MeCN	294 (336)	473	4316	395	8620	0.08
m1d	c-Hex	298 (340)	(401) 415	3645	381 (378)	5315	0.07
	MeCN	296 (340)	494	4650	403	9169	0.06
m1e	c-Hex	299 (351)	406 (418)	3325	387 (387)	3859	0.05
	MeCN	297 (350)	489	4149	407	8122	0.05
m1f	c-Hex	290 (335)	(385) 402	3852	369 (365)	4975	0.11
	MeCN	289 (335)	453	4169	390	7776	0.12
m2a	c-Hex	303 (330)	(367) 381	3731	352 (355)	4056	0.16
	MeCN	304 (330)	429	4399	372	6993	0.14
m2b	c-Hex	306 (342)	(390) 405	3561	373 (369)	4548	0.09
	MeCN	306 (341)	455	3922	397	7347	0.11
m2c	c-Hex	299 (330)	(379) 394	3667	363 (369)	4922	0.14
	MeCN	298 (332)	449	4225	384	7849	0.11
m2e	c-Hex	305 (346)	398 (409)	3169	380 (385)	3776	0.06
	MeCN[f]	304 (344)	361	4050	396	7378	0.07

[a] Fluorescence data are from corrected spectra. [b] Maxima of the long wavelength absorption bands are given in parentheses. [c] Maxima of vibronic shoulders are given in parentheses. [d] The value of $\lambda_{0,0}$ was obtained from the intersection of normalized absorption and fluorescence spectra. The value in parentheses is the $\lambda_{0,0}$ value of the para isomer (from ref 11). [e] $\Delta\nu_{st} = \nu_{abs}(S_0 \rightarrow S_1) - \nu_f$. [f] $f = 4.3 \times 10^{-9} (\nu)d\nu$.

The molecular orbitals of **m1c**−**m1f** were derived by semiempirical INDO/S−SCF−CI (ZINDO) calculations[19] based on the AM1-optimized[20] molecular structures. The highest-occupied molecular orbital (HOMO) and lowest-unoccupied molecular orbital (LUMO) for **m1a**, **m1c**, and **m1e** are shown in Figure 3. More detailed orbitals of **m1a** are available,[6] and those of **m1c** and **m1e** are provided in the Supporting Information. Whereas the LUMO is localized on the stilbene moiety with nearly the same appearance in all three cases, there is a progressive change in the HOMO on going from **m1a** to **m1c** to **m1e**, where the charge density is increased at the nitrogen atom but decreased at the central double bond. Therefore, the HOMO → LUMO transition has an increased charge transfer (CT) character on going from **m1a** to **m1c** to **m1e**, similar to the cases of the para isomers **p1a**−**p1e**. However, it should be

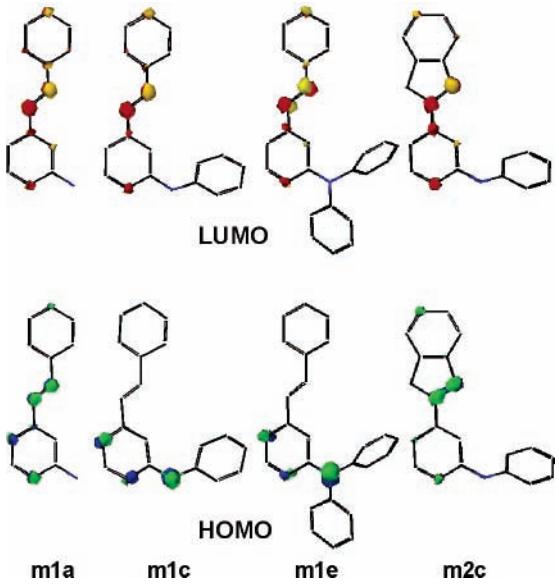

Figure 3. ZINDO-derived HOMO and LUMO for **m1a**, **m1c**, **m1e**, and **m2c**. Only atomic charge densities with 7% or larger contribution are included.

noted that the S_1 state for **m1a**−**m1f** is of significant configuration interactions with the contribution of the HOMO → LUMO configuration to the description of S_1 being only ca. 50%, substantially smaller than that for the para isomers **p1a**−**p1f** (85−95%).[9] It should also be noted that for **m1a**−**m1f** the overall configuration interactions to the description of S_1 is sensitive to the changes in the C−Ph and N−Ph torsional angles. The larger extent of configuration interactions in the meta vs para isomers has been attributed to the loss of symmetry.[6,21]

The electronic absorption spectra of **m2a**−**m2e** resemble those of **m1a**−**m1e**.[22] However, a small but noticeable change in the maximum and oscillator strength for the $S_0 \rightarrow S_1$ absorption band is observed for **m2** vs **m1** (Table 1). As previously demonstrated for **p2** vs **p1**, substitution of the styryl group by indene results in a less planar conformation and more localized frontier orbitals for aminostilbenes.[11] For comparison, the ZINDO-derived HOMO and LUMO for **m2c** are also shown in Figure 3. Whereas the LUMO of **m2c** is not much different from that of **m1**, the charge density in the HOMO mainly locates at the central double bond instead of the nitrogen atom. Furthermore, the contribution of the HOMO → LUMO configuration to the description of S_1 is increased (∼60%) due to a lesser extent of configuration interactions. These differences are expected to lead to a smaller intramolecular CT (ICT) character for the S_1 state. Indeed, the compound series **m2** display a smaller solvent effect than **m1** in their fluorescence properties (vide infra).

Fluorescence Spectra. The fluorescence spectra of **m1c**−**m1f** display diffuse vibrational structures in cyclohexane and become structureless in more polar solvents. Unlike their absorption spectra, the fluorescence maxima show a considerable red shift on going from cyclohexane to acetonitrile. Typical spectra represented by the case of **m1c** are shown in Figure 4. The fluorescence maxima (λ_f), half bandwidth ($\Delta\nu_{1/2}$), and the Stokes shift ($\Delta\nu_{st}$), calculated from the maxima of the S_1 absorption and fluorescence spectra of **m1c**−**m1f** are reported in Table 1 along with the data of **m1a** and **m1b**. The large solvatochromic shifts indicate that the S_1 state possesses a strong ICT character.

The dipole moment of the S_1 state can be estimated from the slope (m_f) of the plot of the energies of the fluorescence maxima

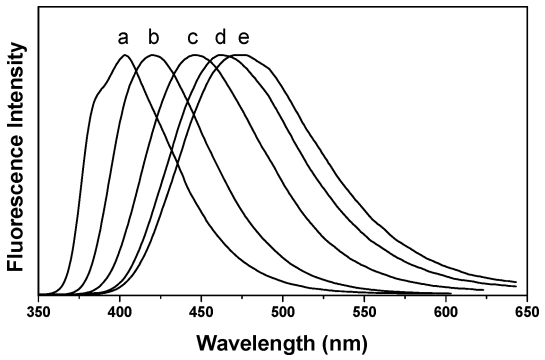

Figure 4. Fluorescence spectra of **m1c** in (a) cyclohexane, (b) toluene, (c) dichloromethane, (d) acetone, and (e) acetonitrile.

TABLE 2: Ground- and Excited-State Dipole Moments for m1 and m2

compd	a (Å)[a]	m_f (cm^{-1})[b]	μ_g (D)[c]	μ_e (D)
m1a	4.26	11135	1.5	10.0
m1b	4.62	10642	1.7	11.1
m1c	4.76	11524	1.1	11.7
m1d	4.84	11560	1.2	12.0
m1e	5.00	12066	0.6	12.6
m1f	4.91	8017	1.4	10.4
m2c	4.67	9040	1.9	10.6

[a] Onsager radius from eq 3 with $d = 0.9$ for **m1b**, 1.0 for **m1a**, **m1c**, **m1d**, and **m1f**, and 1.1 g/cm^3 for **m1e** and **m2c**. [b] Calculated based on eq 1. [c] Calculated by use of ZINDO.

against the solvent parameter Δf according to eq 1[23]

$$\nu_f = -[(1/4\pi\epsilon_0)(2/hca^3)][\mu_e(\mu_e - \mu_g)]\Delta f + \text{constant} \quad (1)$$

where

$$\Delta_f = (\epsilon - 1)/(2\epsilon + 1) - 0.5(n^2 - 1)/(2n^2 + 1) \quad (2)$$

and

$$a = (3M/4N\pi d)^{1/3} \quad (3)$$

where ν_f is the fluorescence maximum, μ_g is the ground-state dipole moment, a is the solvent cavity (Onsager) radius, derived from the Avogadro number (N), molecular weight (M), and density (d), and ϵ, ϵ_0, and n are the solvent dielectric, vacuum permittivity, and the solvent refractive index, respectively. The value of μ_g was calculated using the ZINDO algorithm. Values of the calculated dipole moments of **m1a**−**m1f** are summarized in Table 2. A larger value of μ_e for the *N*-phenyl derivatives **m1c**−**m1e** than **m1a** is consistent with the larger ICT character in the HOMO → LUMO transition in **m1c**−**m1e** vs **m1a** (Figure 3). It should also be noted that the values of μ_e for the meta derivatives are similar in magnitude to those for the corresponding para isomers. Similar phenomena have been observed for meta and para donor−acceptor-substituted benzenes.[24]

The parameters of the fluorescence spectra for the double-bond constrained analogues **m2** are also reported in Table 1. With the same amino substituent, the fluorescence maxima for **m2** vs **m1** are blue shifted with a slightly smaller half bandwidth. As indicated by the values of λ_{00}, the S_1 state of **m2** is of higher energy. Furthermore, the magnitude of the red shift in fluorescence spectrum on going from cyclohexane to acetonitrile is also smaller for **m2**, indicating a weaker ICT character of the S_1 state. This is evidenced by the smaller excited-state dipole moment for **m2c** vs **m1c** (Table 2).

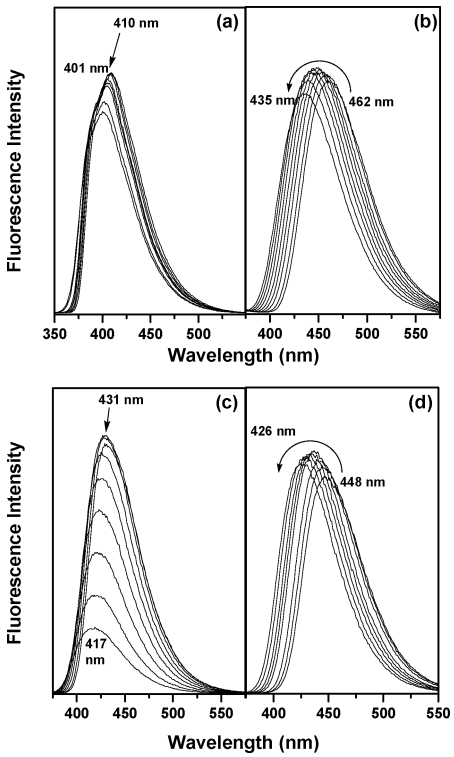

Figure 5. Temperature dependencies of the fluorescence spectra of **m1c** in (a) MCH and (b) MTHF and those of (c) **p1c** and (d) **p1e** in MTHF at 20-K intervals between 180 and 340 K.

The temperature dependence of the fluorescence spectra of **m1b**, **m1c**, **m1e**, and **m2c** was studied in methylcyclohexane (MCH) and 2-methyltetrahydrofuran (MTHF) between 180 and 340 K. The spectra of **m1c** are representative and shown in Figure 5. The fluorescence intensity for all cases in both solvents is rather insensitive to the temperature, but a blue shift of the spectra is observed upon raising the temperature. For **m1b**, **m1c**, and **m1e**, the shift is small (7−9 nm) in MCH, but it is as large as 27−30 nm in MTHF from 180 to 340 K. The corresponding spectral shift is smaller for **m2c**, which is 6 and 20 nm in MCH and MTHF, respectively. A small blue shift of the fluorescence spectra for **ple** in hexane upon raising the temperature was also observed.[9] For comparison, the temperature-dependent fluorescence spectra for **p1c** and **ple** in MTHF are shown in Figure 5. While the size of spectral shift is significant for **ple** (22 nm), it is smaller for **p1c** (14 nm). The large quenching of fluorescence intensity upon raising the temperature for **plc** is consistent with the presence of isomerization in the S_1 state.[9] In contrast, the lack of large changes in fluorescence intensity for 3-aminostilbenes upon changing the temperature indicates the absence of such an activated nonradiative decay process for S_1.

Quantum Yields and Lifetimes. Fluorescence quantum yields and lifetimes (τ_f) for **m1a**−**m1f** and **m2a**−**m2e** in cyclohexane and acetonitrile are given in Table 3 along with the rate constants for radiative ($k_f = \Phi_f/\tau_f$) and nonradiative ($k_{nr} = (1 - \Phi_f)/\tau_f$) decays. For all cases, the Φ_f values decrease on going from cyclohexane to acetonitrile. All decays can be well fit by single-exponential functions, and the fluorescence lifetimes are generally longer in acetonitrile than in cyclohexane. The introduction of *N*-methyl and *N*-phenyl groups to **m1a** reduces the fluorescence quantum yield in the order of **m1a** > **m1f** > **m1b** > **m1c** > **m1d** ≥ **m1e**. There is only a small difference in Φ_f between **m1f** and **m1a**, consistent with their similarities in both absorption and fluorescence spectra. A decrease in k_f and/or an increase in k_{nr} account for the decrease in Φ_f with increasing solvent polarity or upon N substitutions. With the same amino substituent, the values of Φ_f are nearly identical for **m1** and **m2** in cyclohexane, but they are larger for **m2** vs **m1** in acetonitrile. Such a difference in Φ_f between the two compound series results from changes in both k_f and k_{nr}. For further comparison, the fluorescence quantum yields for **m1** and **m2** in THF and dichloromethane were also determined.[22] As depicted in Figure 6, a larger difference in Φ_f between **m1** and **m2** was observed in these medium polarity solvents.

TABLE 3: Quantum Yields for Fluorescence (Φ_f) and Photoisomerization (Φ_{tc}), Fluorescence Decay Times (τ_f), Rate Constants for Fluorescence Decay (k_f), and Nonradiative Decay (k_{nr}) for m1 and m2 in Solution

compd	solvent	Φ_f	Φ_{tc}	τ_f (ns)[a]	k_f (10^8 s^{-1})	k_{nr} (10^8 s^{-1})
m1a	c-Hex[b]	0.78	0.09	7.5	1.0	0.3
	MeCN	0.55	0.23[b]	11.7[b]	0.5	0.4
m1b	c-Hex[c]	0.72	0.08	12.5	0.6	0.2
	MeCN	0.30		13.1	0.2	0.5
m1c	c-Hex	0.57		8.7	0.7	0.5
	CH_2Cl_2	0.29	0.38			
	MeCN	0.17		7.4	0.2	1.1
m1d	c-Hex	0.46		8.8	0.5	0.6
	CH_2Cl_2	0.14	0.40			
	MeCN	0.10		8.4	0.1	1.1
m1e	c-Hex	0.17		6.7	0.3	1.2
	CH_2Cl_2	0.17	0.37			
	MeCN	0.14		11.7	0.1	0.7
m1f	c-Hex	0.70		9.4	0.7	0.4
	CH_2Cl_2	0.45	0.27			
	MeCN	0.44		11.9	0.4	0.5
m2a	c-Hex	0.81		6.6	1.2	0.3
	MeCN	0.68		14.1	0.5	0.2
m2b	c-Hex	0.87		10.3	0.8	0.1
	MeCN	0.43		13.1	0.3	0.4
m2c	c-Hex	0.58		10.0	0.6	0.4
	MeCN	0.21		11.2	0.2	0.7
m2e	c-Hex	0.17		5.0	0.3	1.7
	MeCN	0.16		9.4	0.2	0.9

[a] The value of τ_f was determined with excitation and emission around the spectral maxima, unless otherwise noted. [b] Data from ref 6. [c] Data from ref 7.

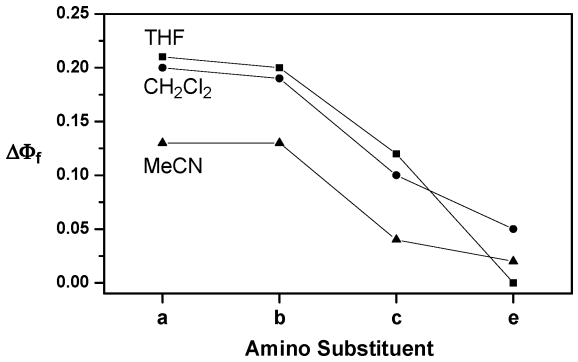

Figure 6. Solvent-dependent difference of Φ_f between **m2** and **m1** ($\Delta\Phi_f = \Phi_f$ (**m2**) − Φ_f (**m1**)).

In addition to fluorescence quantum yields, quantum yields for trans → cis photoisomerization (Φ_{tc}) of **m1c**−**m1f** in dichloromethane are reported in Table 3. By assumption that the decay of the perpendicular p* state yields a 1:1 ratio of trans and cis isomers, the sum of the fluorescence and isomerization quantum yields ($\Phi_f + 2\Phi_{tc}$) for **m1c**−**m1f** equals 1 within the experimental error, as are the cases of **m1a** and **m1b**. This indicates that the decrease in Φ_f is simply compensated by the increase in Φ_{tc} or vice versa among **m1a**−**m1f** and other decay pathways such as internal conversion are

unimportant in accounting for the excited decays of these 3-aminostilbenes.

Discussion

To understand the *m*- vs *p*-amino conjugation effect, we need to understand first the difference in electronic properties between **m1a** and **p1a**, which has mainly been attributed to the difference in molecular (orbital) symmetry.[6] Whereas the $S_0 \rightarrow S_1$ absorption band is essentially a one-electron transition from the HOMO to the LUMO for **p1a**, it arises from extensive configuration interactions in the case of **m1a** due to the loss of symmetry. On the basis of the weak (i.e., low oscillator strength) $S_0 \rightarrow S_1$ band, long fluorescence lifetimes, and low fluorescence rate constants, **m1a** should possess a S_1 state of mixed $^1L_a/^1L_b$ nature, in contrast to the pure ^1L_a character of S_1 for **p1a**. Such a difference in S_1 between meta- and para-substituted benzenes, including distyrylbenzene,[25] is well documented.[17,21] The large dipole moment for the S_1 state of **m1a** indicates that it also possesses a significant extent of ICT component. It is interesting to note that the absorption maximum for the $S_0 \rightarrow S_1$ band is at a shorter wavelength for **m1a** vs **p1a** (e.g., 329 vs 332 nm in hexane), but the opposite trend was found for the fluorescence maximum (e.g., 387 vs 380 nm in hexane), leading to comparable energies for the (0−0) transitions (e.g., 356 vs 354 nm in hexane).[6] In other words, the decrease of the S_1 energy by the configuration interaction-induced excited-state splitting in **m1a** is similar in magnitude to that by the mesomeric interactions in **p1a**. Despite the low fluorescence rate constants, **m1a** displays high fluorescence quantum yields. This is attributed to the inefficient nonradiative decays of the singlet photoisomerization reaction and the $S_1 \rightarrow T_1$ intersystem crossing. The former is nearly inhibited due to the presence of a high torsional barrier (>7 kcal/mol), and the latter conforms to the ^1L_b nature of S_1 and accounts for the low photoisomerization quantum yields (i.e., $\Phi_{isc} \approx 2\Phi_{tc}$).[6]

The introduction of *N*-phenyl groups in **m1a** results in a red shift of the $S_0 \rightarrow S_1$ band along with a reduction in the oscillator strength (Table 1). In contrast, the maxima of the more intense absorption bands near 300 nm are either unchanged or blue shifted (Figure 2a). As a result, the energy gap between the S_1 state and the more allowed upper excited states become larger on going from **m1a** to **m1c** to **m1e**. This might lead to a smaller degree of intensity borrowing (or $^1L_a/^1L_b$ mixing) for the $S_0 \rightarrow S_1$ transition, which accounts for the decrease in oscillator strength along the series. Likewise, the $S_1 \rightarrow S_0$ optical transition becomes less allowed, corresponding to lower fluorescence rate constants (Table 3). Nonetheless, the dipole moment of S_1 continues to increase (Table 2), as is the case of the para isomers,[9] indicating that the ICT process is not affected. While the extent of spectral shift induced by *N*-phenyl substitutions is smaller for the meta than for the para derivatives in both absorption and fluorescence, **m1c**−**m1f** possess a value of λ_{00} similar to the corresponding para isomers **p1c**−**p1f**, resembling the pairs of **m1a** and **pla**. We can thus conclude that the stabilization of S_1 for **m1a** and **p1a** by *N*-phenyl substituents is similar in magnitude.

When compared with its effect on **pla**, *N*-methyl substituents appear to cause a larger stabilization of S_1 for **m1a** (Table 1). We previously reported that **p1b** and **p1c** have similar values of λ_{abs}, λ_f, and λ_{00} in nonpolar hexane solvent, indicating that the hyperconjugation interactions of the dimethylamino group are comparable to the π-conjugation interactions of the anilino group with the stilbene fluorophore.[11] However, the values of λ_{abs}, λ_f, and λ_{00} are all larger for **m1b** than for **m1c**, indicating that the dimethylamino group causes a larger splitting of S_1 than the anilino group does in 3-aminostilbenes. The values of λ_{abs}, λ_f, and λ_{00} for **m1b** are instead closer to those for **m1d**. A stronger splitting of the excited states in **m1b** could also account for the presence of a blue-shifted band at ~280 nm, which is not observed for the other 3-aminostilbenes (Figure 2a). It is known that the magnitude of electronic coupling between the segments in meta-conjugated systems can be very different in the ground vs excited states. It is often small in the ground state but is greatly enhanced in the electronically excited states.[14] To this end, it appears that in the ground-state aminostilbenes **m1a**−**m1f** already have significant electronic interactions between the amino and the stilbene groups. This might be associated with the amino nitrogen that participates in prominent ICT.[21,26]

Aminostilbenes **m1a**−**m1f** are expected to exist as mixtures of conformers as a consequence of rotation about the styrenyl−phenyl C−C and/or amino−stilbenyl C−N single bonds. However, previous conformational studies on **m1a**, **m1b**, **p1c**, **p1d**, and **p1f** have suggested that the conformers in these species have similar absorption and fluorescence spectra.[6,7,9] The same conclusion could apply to the cases of **m1c**−**m1f**, on the basis of the similar values of $\Delta\nu_{1/2}$ (Table 1), the independence of fluorescence spectra on excitation wavelength,[22] and the single-exponential fluorescence decays in all cases.

The photoisomerization quantum yield for **m1** increases at the expense of the fluorescence yield (i.e., $\Phi_f + 2\Phi_{tc} \approx 1.0$ for **m1a**−**m1f**) with *N*-phenyl and/or *N*-methyl substitutions, a phenomenon different from the case of the para isomers. Since **m1a** undergoes photoisomerization via the triplet state due to a high torsional barrier and *N*-phenyl substitutions should further raise the barrier,[6,9] we expect that **m1b**−**m1f** also possess a high barrier for the singlet photoisomerization. This expectation is indeed consistent with the slight temperature dependence of the fluorescence intensity for **m1c** and **m1e** as well as for **m1a** and **ple** (Figure 5). Accordingly, the double-bond torsional relaxation in S_1 is negligible, and the observed photoisomerization reactions should take place in the triplet state. The quantum yields and rate constants for intersystem crossing could in turn be estimated from the photoisomerization or fluorescence quantum yields (i.e., $\Phi_{isc} \approx 2\Phi_{tc} \approx (1 - \Phi_f)$ and $k_{isc} \approx \Phi_{isc}/\tau_f$). It should be noted that the increase in Φ_{tc} on going from **m1a** to **m1c** to **m1e** results not only from an increase of k_{isc} but also from a decrease of k_f (Table 3). The latter could be mainly attributed to a larger splitting of S_1 that leads to a larger ^1L_b character (vide supra). However, factors that could affect the values of k_{isc} among **m1a**−**m1f** are manifold: (a) The optical transition probability: An increase of the ^1L_b character for the S_1 state of aromatic species could reduce k_{isc} as well as k_f.[17] (b) The S_1-T_1 energy gap: A decrease of the S_1 energy may lead to a decrease in the S_1-T_1 gap,[27] which might increase the Franck−Condon integral between the two states and thus the values of k_{isc}.[6−8] (c) The degree of ICT character for S_1: An increase of k_{isc} for *N*-alkylated anilines vs the parent aniline has been correlated with the increased ICT character for S_1.[28] (d) The number of *N*-phenyl groups: It is known that the phenyl C−H stretching modes play an important role in the $S_1 \rightarrow T_1$ intersystem crossing for anilines,[29] so an increase of the *N*-phenyl group might increase k_{isc}. Indeed, the quantum yield for intersystem crossing also increases on going from aniline to diphenylamine to triphenylamine.[30] Since the factors b−d are expected to affect the para derivatives **p1a**−**p1f** to a similar extent, the difference in k_{isc} between **m1a**−**m1f** and **p1a**−**p1f** should be due to their difference in factor a. This in turn leads

to the conclusion that **p1a**−**p1f** should have larger values of k_{isc} than the corresponding meta isomers. This is indeed supported by the comparison of **m1e** and **ple** (e.g., 1.2×10^8 s^{-1} vs 3×10^8 s^{-1} in cyclohexane). In addition, this conclusion also indicates that the triplet mechanism should not be neglected in accounting for the photoisomerization reaction in **plc** and **p1d**.

The dependence of Φ_f on solvent for **m1a**−**m1f** also results from solvent-dependent values of k_f and k_{nr}, namely, k_f is smaller and k_{nr} is larger in more polar solvents. According to the above discussion, the former could be attributed to a larger stabilization of S_1 in more polar solvents and the latter to a reinforcement of factors a−c. It is interesting to note that the solvent effect on Φ_f is more significant for the *m*- vs *p*-aminostilbenes. Since the variation in k_f on going from cyclohexane to acetonitrile is similar in magnitude for both isomers,[11] the larger solvent effect on Φ_f for the meta isomers should mainly arise from the change in k_{nr}. Since the main nonradiative decay channel for **p1a**−**p1f** and **m1a**−**m1f** have been attributed to the singlet and the triplet photoisomerization reaction, respectively, it appears that intersystem crossing is more sensitive to the solvent polarity than singlet torsional relaxation for aminostilbenes.

A blue shift of the fluorescence spectra upon raising the temperature for **m1b**, **m1c**, and **m1e** is similar to the case of **ple**, which has been attributed to a change in molecular geometry. Indeed, it has been suggested that meta-conjugated systems have a less planar geometry than the para isomers in the S_1 state.[17,31] This might reflect the absence of well-resolved vibrational bands for **m1** even in nonpolar cyclohexane solvent (Figure 4). In addition, temperature-dependent C−Ph torsional motions that lead to spectral shifts have been observed for *trans*-stilbene.[32] As such, the amplitude of torsional motion about the planar equilibrium geometry and in turn the degree of configuration interactions in S_1 for **m1a**−**m1f** might vary to some extent in response to the change of temperature. At lower temperatures, these aminostilbenes might be more planar with a larger ICT character, corresponding to a red-shifted fluorescence. This is supported by a larger temperature-induced spectral shift for **m1** in MTHF vs MCH (Figure 5), because an ICT state will have stronger interactions with more polar solvents. Besides the structural factor, the concomitant change in solvent polarizability and polarity upon changing the temperature should also play a part of role in the observed spectral shift.[32]

Compound series **m2** was investigated to determine the role of the double-bond torsional motion in the decay of S_1 in **m1**. Provided that there is a significant portion of photoisomerization through the S_1 state in **m1**, it would be inhibited in **m2**, leading to a larger value of Φ_f and smaller temperature dependence of fluorescence intensity for **m2** vs **m1**. However, this rationale is valid only if **m1** and **m2** have an S_1 state of similar electronic characters, which is not really true in terms of their ICT properties. Thus, the similarity in Φ_f for **m1** and **m2** in cyclohexane but not in THF, dichloromethane, and acetonitrile (Table 3 and Figure 6) could have two possible explanations: (1) The singlet photoisomerization for **m1** is negligible in cyclohexane but occurring in solvents more polar than cyclohexane. (2) The difference in Φ_f between **m1** and **m2** is simply due to their different rates in intersystem crossing, which is solvent dependent. The second explanation can be understood based on the greater ^1L_b character, smaller S_1-T_1 energy gap, and more prominent ICT (i.e., factors a−c in the previous discussion section) for the S_1 state of **m1** vs **m2**. On the other hand, the first explanation might have difficulties to explain the little dependence of the fluorescence intensity of **m1** on temperature in MTHF, in view of the fact that the polarity of MTHF is similar to that of THF.[33] In addition, even when the double-bond torsion in S_1 is nonnegligible, it is still minor in accounting for the nonradiative decay of S_1 for **m1** in solutions.

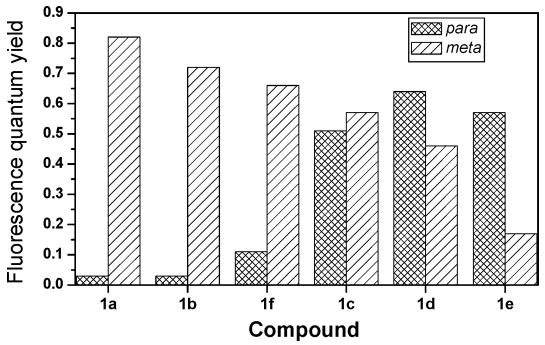

Figure 7. Comparison the *N*-phenyl and *N*-methyl substituent effects on the fluorescence quantum yields of **m1a** (in cyclohexane) and **p1a** (in hexane, data from ref 9).

Concluding Remarks

The "*m*-amino conjugation effect" on the excited-state behavior of *trans*-3-aminostilbene was investigated based on compound series **m1** and **m2**. When compared with the amino conjugation effect on the para isomers (**p1a**−**p1f**),[9,11] the most apparent difference is the opposite trend of fluorescence response, namely, the fluorescence is substantially enhanced for **p1a** upon *N*-phenyl substitution, but it is reduced in the case of **m1a** (Figure 7). This can be attributed to the inherent differences in electronic dynamics between **m1a** and **p1a**. For the fluorescence decay, the $S_1 \rightarrow S_0$ optical transition is less allowed for **m1a** and becomes more forbidden upon *N*-phenyl substitutions. In contrast, the fluorescence decay rate constants are essentially identical for **p1a**−**p1f** in the same solvent.[11] For the nonradiative decay, the $S_1 \rightarrow T_1$ intersystem crossing is predominant in the case of **m1a** and becomes more efficient upon *N*-phenyl substitutions. Although intersystem crossing is also faster in **p1c**−**p1e** relative to **p1a**, the increase in its contribution to the nonradiative decay of S_1 is accompanied by a corresponding decrease in the rate of photoisomerization. Suffice it to say that the "*m*-amino-conjugation effect" reinforces the "*m*-amino effect" on reducing k_f by increasing the ^1L_b character for S_1 and highlights the *N*-phenyl-induced intersystem crossing from the "amino-conjugation effect". This study has provided new insights not only into the excited-state behavior of substituted *trans*-stilbenes but also into the position-dependent substituent effects in molecular photochemistry.

Experimental Section

Materials. *trans*-3-Aminostilbenes **m1c**−**m1f** were prepared by palladium-catalyzed amination reactions between *trans*-3-bromostilbene and the corresponding commercially available arylamines. Typical procedures have been previously reported for the synthesis of the para isomers **p1c**−**p1f**.[9] The synthesis of double-bond constrained analogues **m1a**−**m2c** and **m2e** also followed the same strategy as has been reported for **p2a**−**p2c** and **p2e**.[11] All new compounds were characterized by ^1H NMR, ^{13}C NMR, MS, IR, and/or elemental analysis. These data are provided as Supporting Information. Solvents for spectra and quantum yield measurements all were HPLC grade (TEDIA) and used as received.

Methods. Electronic spectra were recorded at room temperature. UV spectra were measured on a Jasco V-530 double-

beam spectrophotometer. Fluorescence spectra were recorded on a PTI QuantaMaster C-60 spectrofluorometer and corrected for nonlinearity in the response of the detector. The optical density of all solutions was about 0.1 at the wavelength of excitation. It should be noted that, unlike the uncorrected spectra previously reported in refs 9 and 11, the fluorescence spectra reported herein have been corrected for the response of the detector. The fluorescence spectra at other temperature were measured in an Oxford OptistatDN cryostat with an ITC502 temperature controller. A N_2-bubbled solution of phenanthrene ($\Phi_f = 0.13$ in cyclohexane)[34] was used as a standard for the fluorescence quantum yield determinations of aminostilbenes under N_2-bubbled conditions with solvent refractive index correction. An error of ±10% is estimated for the fluorescence quantum yields. Fluorescence decays were measured at room temperature by means of a PTI Timemaster apparatus with a gated hydrogen arc lamp using a scatter solution to profile the instrument response function. The goodness of nonlinear least-squares fit was judged by the reduced χ^2 value (<1.2 in all cases), the randomness of the residuals, and the autocorrelation function. Quantum yields of photoisomerization were measured on optically dense degassed solutions ($\sim 10^{-3}$ M) at 313 nm using a 75-W Xe arc lamp and monochromator. *trans*-Stilbene was used as a reference standard ($\Phi_{tc} = 0.50$ in hexane).[35] The extent of photoisomerization (<10%) was determined using HPLC analysis (Waters 600 Controller and 996 photodiode array detector, Thermo APS-2 Hypersil, heptane and ethyl acetate mixed solvent) without back-reaction corrections. The reproducibility error was <10% of the average. MOPAC-AM1 and INDO/S−CIS−SCF (ZINDO) calculations were performed on a personal computer using the algorithms supplied by the package of Quantum CAChe Release 3.2, a product of Fujitsu Limited.

Acknowledgment. Financial support for this research was provided by the National Science Council of Taiwan, ROC.

Supporting Information Available: Characterization data for new compounds; a full table of fluorescence quantum yields; UV−vis absorption spectra of **m2** in cyclohexane; ZINDO-derived frontier orbitals for **m1c**, **m1e**, and **m2c**; solvatofluorochromic plots for **m1a**−**m1f** and **m2c**; fluorescence spectra of **m1** and **m2** in hexane and acetonitrile recorded by changing the excitation wavelengths (PDF). This material is available free of charge via the Internet at http://pubs.acs.org.

References and Notes

(1) (a) Saltiel, J.; Charlton, J. L. *Rearrangements in Ground and Excited States*; de Mayo, P., Ed, Academic Press: New York, 1980; Vol. 3, pp 25−89. (b) Saltiel, J., Sun, Y.-P. *Photochromism, Molecules and Systems*; Dürr, H., Bouas-Laurent, H., Eds.; Elsevier: Amsterdam, 1990; pp 64−164. (c) Waldeck, D. H. *Chem. Rev.* **1991**, *91*, 415−436. (d) Görner, H.; Kuhn, H. J. *Adv. Photochem.* **1995**, *19*, 1−117.

(2) (a) Meier, H. *Angew. Chem., Int. Ed. Engl.* **1992**, *31*, 1399−1420. (b) Simeonov, A.; Matsushita, M.; Juban, E. A.; Thompson, E. H. Z.; Hoffman, T. Z.; Beuscher IV, A. E.; Taylor, M. J.; Wirsching, P.; Rettig, W.; McCusker, J. K.; Stevens, R. C.; Millar, D. P.; Schultz, P. G.; Lerner, R. A. Janda, K. D. *Science* **2000**, *290*, 307−313. (c) Papper, V.; Likhtenshtein, G. I. *J. Photochem. Photobiol., A* **2001**, *140*, 39−52.

(3) (a) Saltiel, J.; Megarity, E. D.; Kneipp, K. G. *J. Am. Chem. Soc.* **1966**, *88*, 2336−2338. (b) Saltiel, J. *J. Am. Chem. Soc.* **1967**, *89*, 1036−1037.

(4) Saltiel, J.; Marinari, A.; Chang, D. W.-L.; Mitchener, J. C.; Megarity, E. D. *J. Am. Chem. Soc.* **1979**, *101*, 2982−2996.

(5) Lewis, F. D.; Yang, J.-S. *J. Am. Chem. Soc.* **1997**, *119*, 3834−3835.

(6) Lewis, F. D.; Kalgutkar, R. S.; Yang, J.-S. *J. Am. Chem. Soc.* **1999**, *121*, 12045−12053.

(7) Lewis, F. D.; Weigel, W. *J. Phys. Chem. A* **2000**, *104*, 8146−8153.

(8) Lewis, F. D.; Weigel, W.; Zuo, X. *J. Phys. Chem. A* **2001**, *105*, 4691−4696.

(9) Yang, J.-S.; Chiou, S.-Y.; Liau, K.-L. *J. Am. Chem. Soc.* **2002**, *124*, 2518−2527.

(10) Yang, J.-S.; Liau, K.-L.; Wang, C.-M.; Hwang, C.-Y. *J. Am. Chem. Soc.* **2004**, *126*, 12325−12335.

(11) Yang, J.-S.; Wagn, C.-M.; Hwang, C.-Y.; Liau, K.-L.; Chiou, S.-Y. *Photochem. Photobiol. Sci.* **2003**, *2*, 1225−1231.

(12) (a) Zimmerman, H. E. *J. Am. Chem. Soc.* **1995**, *117*, 8988−8991. (b) Zimmerman, H. E. *J. Phys. Chem. A* **1998**, *102*, 5616−5621.

(13) Tomonari, M.; Ookubo, N. *Chem. Phys. Lett.* **2003**, *376*, 504−514.

(14) (a) Gaab, K. M.; Thompson, A. L.; Xu, J.; Martinez, T. J.; Bardeen, C. J. *J. Am. Chem. Soc.* **2003**, *125*, 9288−9289. (b) Thompson, A. L.; Gaab, K. M.; Xu, J.; Bardeen, C. J.; Martinez, T. J. *J. Phys. Chem. A* **2004**, *108*, 671−682.

(15) Melinger, J. S.; Pan, Y.; Kleiman, V. D.; Peng, Z.; Davis, B. L.; McMorrow D.; Lu, M. *J. Am. Chem. Soc.* **2002**, *124*, 12002−12012.

(16) Nakano, M.; Takahata, M.; Yamada, S.; Yamaguchi, K.; Kishi, R.; Nitta, T. *J. Chem. Phys.* **2004**, *120*, 2359−2367.

(17) (a) Nijegorodov, N. I.; Downey, W. S.; Danailov, M. B. *Spectrochim. Acta, A* **2000**, *56*, 783−795. (b) Mabbs, R.; Nijegorodov, N.; Downey, W. S. *Spectrochim. Acta, A* **2003**, *59*, 1329−1339.

(18) (a) Halim, M.; Pillow, J. N. G.; Samuel, D. W.; Burn, P. L. *Adv. Mater.* **1999**, *11*, 371−374. (b) Díez-Barra, E.; García-Martínez, J. C.; Merino, S.; del Rey, R.; Rodríguez-López, J.; Sánchez-Verdú, P.; Tejeda, J. *J. Org. Chem.* **2001**, *66*, 5664−5670. (c) Tammer, M.; Horsburgh, L.; Monkman, A. P.; Brown, W.; Burrows, H. D. *Adv. Funct. Mater.* **2002**, *12*, 447−454. (d) Pogantsch, A.; Mahler, A. K.; Hayn, G.; Saf, R.; Stelzer, F.; List, E. J. W.; Brédas, J.-L.; Zojer, E. *Chem. Phys.* **2004**, *297*, 143−151.

(19) Zerner, M. C.; Leow, G. H.; Kirchner, R. F.; Mueller-Westerhoff, U. T. *J. Am. Chem. Soc.* **1980**, *102*, 589−599.

(20) Dewar, M. J. S.; Zoebisch, E. G.; Healy, E. F.; Stewart, J. J. P. *J. Am. Chem. Soc.* **1985**, *107*, 3902−3909.

(21) Findley, G. L.; Carsey, T. P.; McGlynn, S. P. *J. Am. Chem. Soc.* **1979**, *101*, 4511−4517.

(22) See Supporting Information.

(23) Baumann, W.; Bischof, H.; Fröhling, J.-C.; Brittinger, C.; Rettig, W.; Rotkiewicz, K. *J. Photochem. Photobiol., A* **1992**, *64*, 49−72.

(24) Sinha, H. K.; Yates, K. *J. Am. Chem. Soc.* **1991**, *113*, 6062−6067.

(25) Meier, H.; Zertani, R.; Noller, K.; Oelkrug, D.; Krabichler, G. *Chem. Ber.* **1986**, *119*, 1716−1724.

(26) Murrell, J. N.*The Theory of the Electronic Spectra of Organic Molecules*; John Wiley and Sons: New York, 1963.

(27) Wilhelm, H. E.; Gebert, H.; Regenstein, W. *Z. Naturforsch.* **1997**, *52a*, 837−842.

(28) Seliskar, C. J.; Khalil, O. S.; McGlynn, S. S. in *Excited States I*; Lim, E. C., Ed.; Academic Press: New York, 1974; pp 231−294.

(29) Scheps, R.; Florida, D.; Rice, S. A.*J. Chem. Phys.* **1974**, *61*, 1730−1747.

(30) (a) Kasha, M.; Rawls, H. R.; El-Bayoumi, M. A. *Pure Appl. Chem.* **1965**, *11*, 371−392. (b) Malkin, J. *Photophysical and Photochemical Properties of Aromatic Compounds*; CRC Press: Boca Raton, 1992.

(31) Karabunarliev, S.; Baumgarten, M.; Tyutyulkov, N.; Müllen, K. *J. Phys. Chem.* **1994**, *98*, 11892−11901.

(32) Saltiel, J.; Choi, J.-O.; Sears, D. F., Jr.; Eaker, D. W.; Mallory, F. B.; Mallory, C. W. *J. Phys. Chem.* **1994**, *98*, 13162−13170.

(33) Macus, Y. *Chem. Soc. Rev.* **1993**, 409−416.

(34) Berlman, I. B. *Handbook of Fluorescence Spectra of Aromatic Molecules*, 2nd ed.; Academic Press: New York, 1971.

(35) Malkin, S.; Fischer, E. *J. Phys. Chem.* **1964**, *68*, 1153−1163.